

Article

Lattice Relaxation Forward Negative Coulomb Drag in Hopping Regime

Dongyang Liu ^{1,2} , Jiawei Wang ^{1,2,3,*}, Chong Bi ¹, Mengmeng Li ¹ , Nianduan Lu ^{1,2}, Zhekai Chen ⁴ and Ling Li ^{1,2}

¹ Key Laboratory of Microelectronic Devices & Integrated Technology, Institute of Microelectronics of Chinese Academy of Sciences, Beijing 100029, China; liudongyang@ime.ac.cn (D.L.); bichong@ime.ac.cn (C.B.); limengmeng@ime.ac.cn (M.L.); lunainduan@ime.ac.cn (N.L.); lingli@ime.ac.cn (L.L.)

² University of Chinese Academy of Sciences, Beijing 100049, China

³ Peng Cheng Laboratory, Department of Mathematics and Theories, No. 2, Xingke 1st Street, Nanshan, Shenzhen 518055, China

⁴ School of Physics Sciences, Nankai University, Tianjin 300071, China; wind_runner@foxmail.com

* Correspondence: wangjiawei@ime.ac.cn

Abstract: Quasi-particle formed by electron and the dressed deformed lattice is important to accurately interpret the properties of various disordered/amorphous materials. However, a unified understanding of the drag effect, in particular the negative Coulomb drag in hopping systems, remains an open challenge. This work proposes a theoretic framework to account for both positive and negative Coulomb drag in dual-1D-hopping systems by considering both the electron-electron correlation and the electron-phonon correlation. It is found that lattice relaxation in the active line of the hopping system may give rise to an inverse energetic pumping force in the passive line, causing negative Coulomb drag. The mobility of the negative coulomb drag can approach the scale of $10^{-5}\text{cm}^2\text{V}^{-1}\text{s}^{-1}$, especially at low temperature, high carrier-density, and narrow inter-spacing separation. More intriguingly, the positive drag could be recovered by varying the energy fluctuation and suppressing the electron-phonon interactions, but with a much lower magnitude. Our work could serve as a universal model for the Coulomb drag effect in the hopping system.

Keywords: hopping regime; negative coulomb drag; positive coulomb drag



Citation: Liu, D.; Wang, J.; Bi, C.; Li, M.; Lu, N.; Chen, Z.; Li, L. Lattice Relaxation Forward Negative Coulomb Drag in Hopping Regime. *Electronics* **2022**, *11*, 1273. <https://doi.org/10.3390/electronics11081273>

Academic Editor: Qing-Tai Zhao

Received: 25 February 2022

Accepted: 12 April 2022

Published: 17 April 2022

Publisher's Note: MDPI stays neutral with regard to jurisdictional claims in published maps and institutional affiliations.



Copyright: © 2022 by the authors. Licensee MDPI, Basel, Switzerland. This article is an open access article distributed under the terms and conditions of the Creative Commons Attribution (CC BY) license (<https://creativecommons.org/licenses/by/4.0/>).

1. Introduction

The Coulomb drag effect originated from the broken electron-hole symmetry and electron interactions [1,2]. It can be significant in a mesoscopic system of two interacting conducting circuits, where the current in one circuit could drive the motion of carriers in the other one due to the momentum transfer caused by electron interactions. This phenomenon becomes more evident in low-dimensional systems such as Luttinger liquid [3], quantum wire structures [4–7], and graphene layers [8,9]. Existing theoretical [10–14] and experimental research [15–20] are mostly based on the theory that the momentum and energy transfer occur between spatially separated electron gases due to the Coulomb coupling. Therefore, high mobility materials or structures were usually employed to study this effect. Meanwhile, the concept of momentum transfer is not applicable for the low mobility systems where charge transport occurs in the hopping regime among localized states. Only a limited volume of research has discussed possible mechanisms for realizing the hopping drag effect in such a system. M. E. Raikh et al. [21] employed a charge pumping mechanism in the structure of two neighboring pairs of sites; by considering the electron-electron interaction, they theoretically realized the directional migration of carriers by the Coulomb drag effect. V. I. Kozub et al. [22] considered the influence of electron-hole pairs, and then a novel negative Coulomb drag [23] by dipole–dipole interactions between the critical resistors in the active and the passive layer was remarkably realized.

Besides the direct Coulombic correlation between electrons, the coupling between the electrons and the surrounding lattice, i.e., the polaron effect [24], is also essential for determining the transport characteristics, especially in materials with relative 'soft' lattice featured by low-frequency vibration modes like organic solids [25]. Due to the finite relaxation time, the deformed lattices usually lag behind the moving electrons [26], forming an effective polarized center that might further modify the other electron's motion. This introduces an effective electron-electron interaction, which should be emphasized in treating the hopping drag problems.

The study of the Coulomb drag effect can be used to explore the physical properties of low-dimensional systems, can be used to detect spontaneous charge fluctuations due to many-body associations [27], and distinguish Fermi liquids from Luttinger liquids [3]. It can also play an important role in designing nanodevices, such as single-electron transistors [28] and quantum cellular automata [29].

2. Methods and Calculation

In this letter, we theoretically predicted the possibility of negative hopping drag by introducing the lattice distortion dressed behind the electron. A reversing electric field could be formed in the passive line with such a polaronic effect, leading to a pumping effect on the electron in the opposite direction. The negative drag effect was derived with the Miller-Abrahams hopping framework [30] under varying parameters, including energetic disorder, lattice relaxation time, and correlation strength. Moreover, the positive drag effect could recur at the decrease of the relaxation time in a rigid lattice but is much weaker than that of the negative one. Here, we present the detailed results, analysis, and discussions about the realization of the hopping drag effect.

Two parallel chains with hopping conduction were assumed with discrete, separated distance, at which scale the interchain tunneling is negligible while the coulomb correlation works [20]. In the system of localized sites, polarons are the main quasi-particles carrying charges [31], which are formed by electrons (holes) dressed with deformed lattices. In systems with soft lattices such as organic semiconductors, the low-frequency phonon modes will lead to strong asynchronization between the electron and the lattice deformation. This is illustrated by the transition process in the configuration coordinate of Figure 1, where the ionization and neutralization of a site in carriers' hopping could proceed in 4 steps [32], (1) the neutral site suddenly accepts an electron after a vertical transition, but the lattice is adiabatic at this moment, and the waiting time for this configuration before the lattice's relaxation is assumed to be τ_1 ; (2) the lattice relaxation occurs, and the ionized site reaches the new equilibrium configuration with duration time τ_2 ; (3) the ionized site loses the electron in a vertical transition, leaving the deformed lattice for a period of time τ_3 ; (4) the deformed lattice restores to the equilibrium position of the neutral site, lasting for a period of τ_4 before accepting a new electron.

An architecture with three adjacent sites in one dimension was used to demonstrate the calculated electron hopping process, as in Figure 2. Solid lines represent hopping sites, red circles represent electrons, and positive marks denote the cloud of deformed lattices. Spatially, the deformed lattice that acts as an effective positive charge will lag behind the electron. The dragging process could be divided into 7 sections, i.e., from Γ_1 to Γ_7 . Among them, Γ_1 to Γ_4 relate to the 4 stages of τ_1 to τ_4 for site 1; Γ_3 to Γ_6 relate to the stages of τ_1 to τ_4 for site 2; while Γ_5 , Γ_6 , and Γ_7 relate to the stages of τ_1 , τ_2 , and τ_3 for site 3, all corresponding to the transitions process defined in Figure 1. Due to the motion of electrons and quasi-particles, energetic correlation effects will be triggered in the passive line in these 7 sections.

As demonstrated in the insert figure of Figure 2, let us define that site 1 of the active line is in the τ_3 stage, while site 2 is in its τ_1 , i.e., the electron just drifts from site 1 to 2. Negative electrons will negatively modulate the electrostatic potential on the nearby site in the passive line; therefore, the electrostatic energy of an electron on the site will rise. When it comes to the positive charged deformed lattice, oppositely, the nearby site in the passive

line is mediated by positive electrostatic potential, and the on-site electrostatic energy of an electron will decrease. Thus, negative electrons in the active layer and positively deformed lattice induce opposite energy fluctuations to electrons in the passive layer. Due to the coulombic correlations, the electron on site 2 would uplift the energy of the parallel site 2' along the passive line. In contrast, the unrelaxed deformed lattice on site 1 has an inverse energy influence in the passive line compared with the electron, which lowers the site energy in the parallel site 1'. Consequently, an effective electric field in the opposite direction with the active line's drift current forms between sites 1' and 2' in the passive line. An electron at site 2' in the passive line has a greater probability of transitioning to site 1' compared to site 3', making it possible to generate a macroscopically opposite current in the passive line contrasted to the active line.

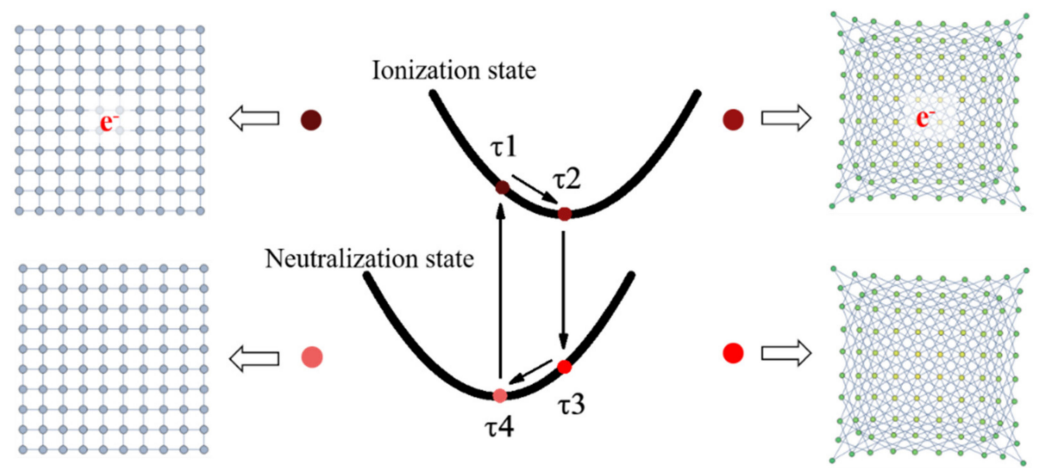


Figure 1. The configuration coordinate for the electron transfer process. τ_1 relates to the ionization of a site in which the phonon is adiabatic without lattice deformation; τ_2 relates to the relaxation of the charged site with the lattice deformation process for a new equilibrium state; τ_3 relates to the neutralization of the charged site in which the phonon is adiabatic, and lattice deformation remains; τ_4 relates to the release of the deformation of the lattice.

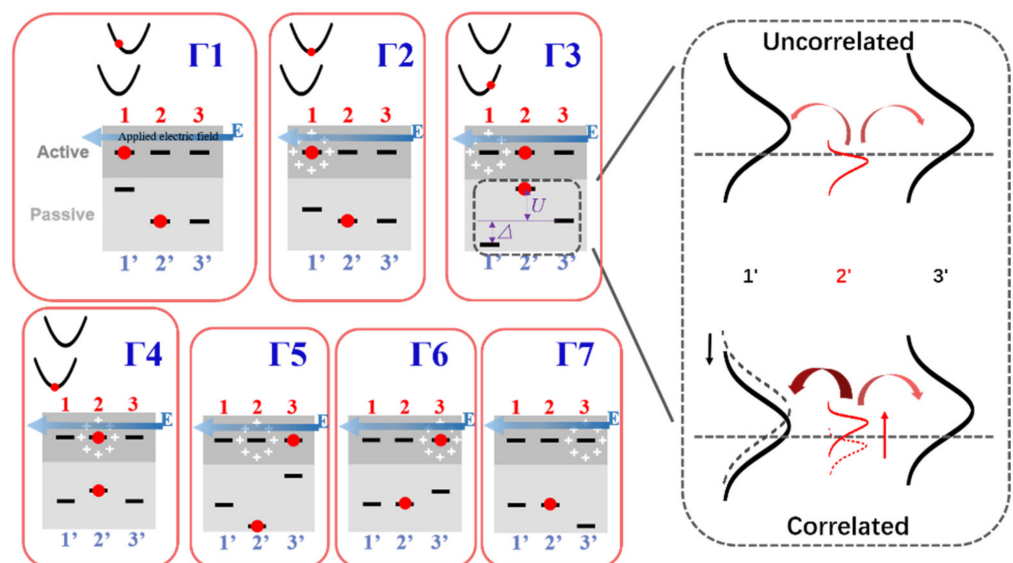


Figure 2. The electron and quasi-particle transfer process in the active line and the energy fluctuation in the passive line. The insert figure shows the site energy in the passive line described by a Gaussian distribution. “Uncorrelated” and “Correlated” respectively indicate the states before and after being affected by the deformed lattices and the electrons in the active line.

The negative drag current was further calculated within the hopping framework by employing the Miller-Abrahams hopping rate [30]

$$v_{ij} = v_0 \times \exp\left(-\frac{2r_{ij}}{\alpha} - \frac{\varepsilon_j - \varepsilon_i + |\varepsilon_i - \varepsilon_j|}{2kT}\right) \tag{1}$$

where v_{ij} is the hopping rate from site i to site j , v_0 is the attempt-to-escape frequency, r_{ij} is the inter-site distance, α is the localization length of charge carriers, ε_i and ε_j are the carrier energies on sites i and j , respectively, k is the Boltzman constant, and T is the temperature.

Our calculation sequence is to determine the Fermi level first, calculate the electron escape frequency in the passive line v_p , then calculate the electron escape frequency in the active line v_a , and finally calculate the drag current $v_{negative}$. As for the electron mobility, it can be calculated by the escape frequency:

$$D = v \times \alpha^2 \tag{2}$$

$$D = \frac{k \times T}{q} \times \mu \tag{3}$$

where v is the hopping rate, D is the diffusion coefficient, and μ is the mobility.

The Gaussian density of states (DOS) is introduced to depict the system disorder [30]

$$g(\varepsilon) = \frac{N}{\sigma\sqrt{2\pi}} \times \exp\left(-\frac{\varepsilon^2}{2\sigma^2}\right) \tag{4}$$

where σ is the energy scale of the density of states, and N is the total number of localized sites. The carrier concentration $n = N/1000$ is assumed in our system to determine the Fermi level:

$$n = \int_{-\infty}^{+\infty} g(\varepsilon) \times f(\varepsilon) d\varepsilon \tag{5}$$

where $f(\varepsilon)$ is the Fermi distribution.

As shown in Figure 2, let us assume there is an electron located at site $2'$, whose site energy can be described as $\varepsilon_{2'} = \int \varepsilon N(\varepsilon) f(\varepsilon) d\varepsilon / \int N(\varepsilon) f(\varepsilon) d\varepsilon$; while the unoccupied sites $1'$ and $3'$ are featured by higher expectancy energy, so that $\varepsilon_{1,3'} = \int \varepsilon N(\varepsilon) (1 - f(\varepsilon)) d\varepsilon / \int N(\varepsilon) (1 - f(\varepsilon)) d\varepsilon > \varepsilon_{2'}$. If no coulomb correlation exists, the transition possibilities (or the hopping rates) from site $2'$ to sites $1'$ and site $3'$ will be the same. When correlations are introduced, for instance, at the section of $\Gamma 3$, the hopping rates are no more in equilibrium due to the imbalance in forward and backward hopping barriers' heights, $E_{forward} = \varepsilon_{3'} - (\varepsilon_{2'} + U)$, and $E_{backward} = (\varepsilon_{1'} + \Delta) - (\varepsilon_{2'} + U)$, ref. [33] where U and Δ are the correlation energy from electron and deformed lattice, respectively. Due to the smaller barrier for backward hopping $E_{forward} > E_{backward}$, a negative dragging effect can be shown in this section. The hopping rates and direction in other sections could be obtained similarly, and the total hopping rate is the superposition of all these individual rates.

For simplicity of calculation, we assumed an even distribution of waiting time $\tau_1 = \tau_2 = \tau_3 = \tau_4$. Namely, the drag rate in the passive line is calculated by $v_p = \frac{1}{7}v_{p1} + \frac{1}{7}v_{p2} + \frac{1}{7}v_{p3} + \frac{1}{7}v_{p4} + \frac{1}{7}v_{p5} + \frac{1}{7}v_{p6} + \frac{1}{7}v_{p7}$, where v_{pi} is the hopping frequency of section Γi , defined as $v_{pi} = \frac{v_{pi-left} + v_{pi-right}}{2}$, in which $v_{p1-left}$ represents the rate of hopping from site $2'$ to site $1'$, $v_{p1-right}$ represents the rate of hopping from site $2'$ to site $3'$, and were calculated via

$$v_p = \frac{1}{N - n} \int_{-\infty}^{+\infty} v_{ij} \times (1 - f(\varepsilon)) d\varepsilon \tag{6}$$

$$v_a = \frac{1}{(N-n) \times n} \int_{-\infty}^{+\infty} f(\varepsilon_j) \int_{-\infty}^{+\infty} v_{ij} \times (1-f(\varepsilon_i)) d\varepsilon_i d\varepsilon_j \quad (7)$$

where v_p is the electron escape frequency caused by the energy fluctuations in the passive line, v_a is the electron escape frequency caused by the voltage applied on the active line.

As we theoretically predict, the proposed negative hopping drag might significantly influence the charge transport in soft materials like organic semiconductors, especially in some organic materials with quasi-1D structures. One example is conjugated polymers, where intra-chain hopping is much faster than inter-chain one. Like materials PBTTT and IDTBT, where conductance is mainly dominated by polaronic hopping along the 1D backbone; therefore, correlations among chains might bring drag effect into the charge transport. Another example is the 1D organic conductor formed by charge transfer molecules, drag effect among the 1D chains might have a significant influence on modifying the transport properties of the systems. Our theoretic work might provide pathways and references for further optimizing relevant materials systems' charge transport theoretic framework.

In order to demonstrate the impact of the lattice relaxation time, we set $\tau_1 = \tau_3$, $\tau_2 = \tau_4$, and assumed the ratio of waiting time in the lattice relaxation sections (Section 1, 3, 5, 7 in Figure 2) throughout the entire electron transfer process is τ . Then, v_p is calculated by $v_p = \frac{\tau}{7}(v_{p1} + v_{p3} + v_{p5} + v_{p7}) + \frac{1}{7} \times \frac{7-4\tau}{3}(v_{p2} + v_{p4} + v_{p6})$. Based on these, the diffusion constant D and mobility μ could be further obtained via $D = v \times a^2$, and $D = \frac{k_B T}{q} * \mu$, where a is the inter-site distance. Then the drag current $v_{negative}$ could be defined as

$$v_{negative} = \frac{v_a \times v_p}{v_a + v_p} \quad (8)$$

where $v_{negative}$ is the drag current induced by the active current.

When it comes to a totally rigid lattice or a system with only high-frequency phonon modes, the lattice relaxation time is negligibly short, and lattice deformation and electron move together without any delay between them. When the lattice relaxation disappears, the original seven drag process in Figure 1 becomes three sections in Figure 3a. In such a situation, as shown in Figure 3a, we begin with a charge located at site 1 in the active line and a charge located at site 2' in the passive line. In section Γ_1 , due to the coulombic correlations, the electron on site 1 would uplift the energy of the parallel site 1', the carrier at site 2' has a greater probability of hopping to site 3' than to site 1' as Formula (1). In section Γ_2 , the carrier at site 2' has the same probability of hopping to site 3' than to site 1'. In section Γ_3 , due to the coulombic correlations, the electron on site 3 would uplift the energy of the parallel site 3', the carrier at site 2' has a greater probability of hopping to site 1' than to site 3' as Formula (1), which is completely inverse to section Γ_1 . No macroscopic current is formed considering the whole electron transfer (sections Γ_1 , Γ_2 , and Γ_3). However, when considering a secondary order case, as shown in Figure 3b, the forward hopping charge has some possibility of being further driven forward by the same charge in the active line again. In contrast, the same charge would no longer drive the backward hopping charge. The hopping frequency of positive drag can only be -described as

$$v_p \propto v_{p2} \quad (9)$$

As shown in Figure 4a, the dependency of the negative drag mobility on the temperature T , the correlation strength from electrons (expressed by parameter U), and deformed lattices (expressed by parameter Δ) are displayed. The negative drag mobility decreases with the increase of temperature, showing decreased correlation effect when thermal activation weakens the system disorders' influence. In addition, both the correlations from the electrons (noted as U) and lattices (noted as Δ) correlation strength could effectively determine the strength of the drag effect, shown in Figure 4a. In the Miller-Abrahams hopping framework, the energy difference determines the hopping rate, as shown in Equation (1).

The effect of the parameters U and Δ on the negative coulomb drag hopping rate show the fundamental roles of their interactions in the negative drag process.

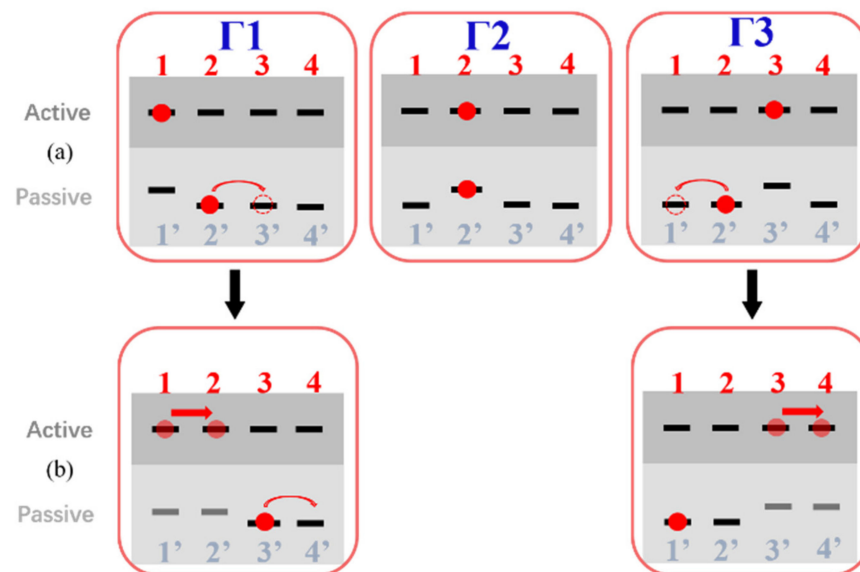


Figure 3. Mechanism for the positive hopping drag without lattice relaxation. (a) When the charge in the active line locates at site 1, a charge carrier at site 2' in the passive line has a larger probability of hopping forward. In contrast, this probability is offset when the charge in the active line moves to site 3 and no net current exists. (b) In a secondary order case, the forward hopping charge has some possibility of being driven forward by the same charge in the active line again, but the same charge would no longer drive the backward hopping charge.

The influence of relaxation time on mobility in the passive line is displayed in Figure 4b. It is evident that there is a positive correlation between the lattice relaxation time τ_3 and the intensity of the negative drag effect and such dependence could be enhanced by increasing the correlation strength either from the electron or the deformed lattice.

Figure 4c shows the dependency of the negative coulomb drag mobility on the degree of disorders of the density of states, with a Gaussian width σ ranging from 0.1 to 0.5 eV. With an increasing degree of disorder, the energy fluctuations in the passive line caused by the deformed lattices and electrons in the active line will be dispersed. Consequently, the negative drag effect will be quenched by the increasing degree of system disorder.

As shown in Figure 4d, when shortening the lattice relaxation time τ_3 to zero, the negative drag effect becomes positive as the coulomb drag mobility is positive. This verifies our theory that the lattice relaxation in the hopping system's active line gives rise to an inverse energetic pumping force in the passive line, causing negative coulomb drag. When ignoring the effect of lattice relaxation in the active line and only considering electron-electron interactions, no negative drag occurs, and at this time, the situation is similar to that in the research [22]. Only positive coulomb drag will occur. In the meantime, we can find that it is a thermal activation process when the effect of the lattice deformation correlation is wiped out. The positive drag is a thermal activation process, while the effect of the lattice deformation correlation is wiped out. The factors leading to the positive drag exist in the negative drag process when τ_3 is finite, while we could see that the positive frequency is approximately two orders smaller than that of negative drag, and therefore it is only a perturbation item.

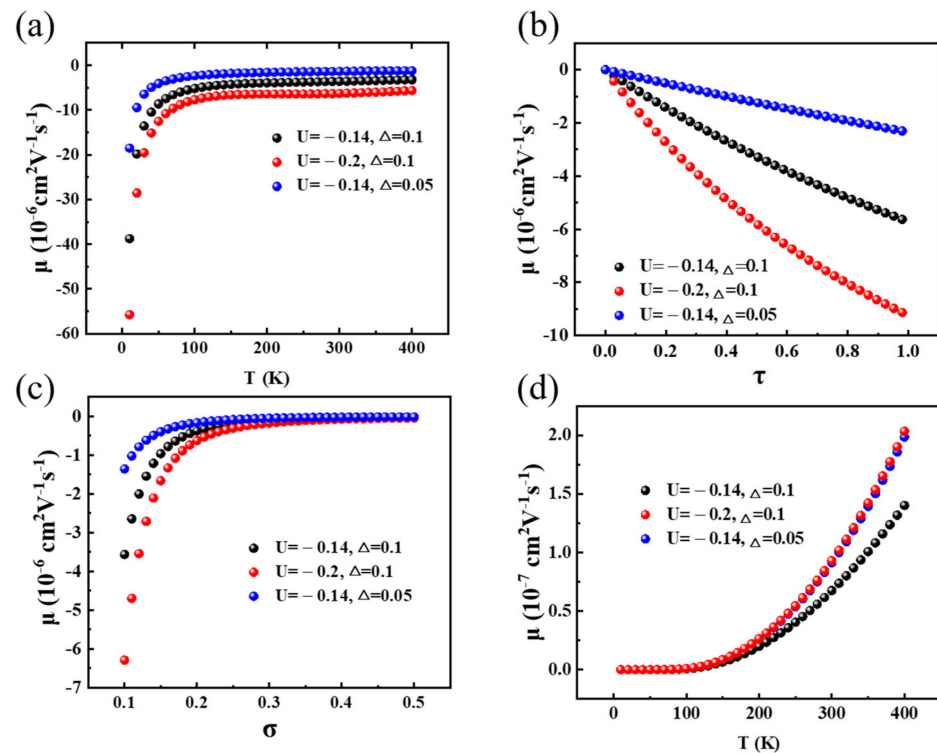


Figure 4. (a) The negative coulomb drag mobility varies with temperature. (b) The negative coulomb drag mobility varies with the ratio of the lattice relaxation time to the total time. (c) The negative coulomb drag mobility varies with the ratio of the disorder. (d) The positive coulomb drag mobility varies with temperature. In this calculation, $v_p = v_{p2}$ is assumed ($\tau = 0$). U and Δ mean the correlation energy of electron-electron and electron-quasiparticle. In this calculation, $\alpha = 10^{-8}$ cm, $v_0 = 10^{12}$ s $^{-1}$, $\sigma = 0.1$ eV. We assume that the voltage drop in two neighboring sites is 0.1 eV.

3. Conclusions

In conclusion, a theory combining correlations from both deformed lattice and electrons is proposed for the prediction of the existence of the negative Coulomb drag effect in the disordered chain. Asynchrony in motions of the electrons and deformed lattice in the active line will introduce energy fluctuations in the passive line, which finally drives the negative hopping transport. When the motions' non-sync is removed, the negative drag effect will be reversed to the positive one but with lower intensity. Meanwhile, the dependency of the negative drag effect on the correlation strength and the degree of system disorder are investigated and discussed within a Miller-Abrahams hopping framework. This letter might provide new possibilities for utilizing the quantum effect from electron-lattice couplings and a pathway for understanding correlations of charge transport in disorder solids like organic semiconductors.

Author Contributions: Validation, C.B., M.L., N.L., Z.C. and L.L.; Writing—original draft, D.L.; Writing—review & editing, J.W. All authors have read and agreed to the published version of the manuscript.

Funding: Please add: This work was supported in part by the National key research and development program (Grant Nos. 2018YFA0208503, 2019YFB2205002, 2021YFB3600704), by the Opening Project of Key Laboratory of Microelectronic Devices and Integrated Technology, Institute of Microelectronics, Chinese Academy of Sciences, and by the National Natural Science Foundation of China (Grant Nos. 61890944, 61725404, 61874134, 61804170, 61821091, 61888102, 61720106013, 61904195, 61404164 and 62004214), by the Beijing Training Project for the Leading Talents in S&T under Grant No. Z151100000315008, by the Strategic Priority Research Program of the Chinese Academy of Sciences (Grant No. XDB30030000, XDB30030300).

Data Availability Statement: Not applicable.

Conflicts of Interest: The authors declare no conflict of interest.

References

1. Narozhny, B.N.; Levchenko, A. Coulomb drag. *Reviews of Modern Physics*. *Rev. Mod. Phys.* **2016**, *88*, 025003. [[CrossRef](#)]
2. Tse, W.-K.; Hu, B.Y.-K.; Hong, J.N.; MacDonald, A.H. Magneto-Coulomb Drag and Hall Drag in Double-Layer Dirac Systems. *Phys. Rev. Lett.* **2019**, *122*, 186602. [[CrossRef](#)] [[PubMed](#)]
3. Laroche, D.; Gervais, G.; Lilly, M.P.; Reno, J.L. 1D-1D Coulomb drag signature of a Luttinger liquid. *Science* **2014**, *343*, 631–634. [[CrossRef](#)] [[PubMed](#)]
4. Badalyan, S.M.; Jauho, A.P. Coulomb drag between a carbon nanotube and monolayer graphene. *Phys. Rev. Res.* **2020**, *2*, 013086. [[CrossRef](#)]
5. Mitra, R.; Sahu, M.R.; Watanabe, K.; Taniguchi, T.; Shtrikman, H.; Sood, A.K.; Das, A. Anomalous Coulomb drag between InAs nanowire and graphene heterostructures. *Phys. Rev. Lett.* **2020**, *124*, 116803. [[CrossRef](#)]
6. Laroche, D.; Gervais, G.; Lilly, M.P.; Reno, J.L. Positive and negative Coulomb drag in vertically integrated one-dimensional quantum wires. *Nat. Nanotechnol.* **2011**, *6*, 793. [[CrossRef](#)]
7. Klesse, R.; Stern, A. Coulomb drag between quantum wires. *Phys. Rev. B* **2000**, *62*, 16912. [[CrossRef](#)]
8. Ho, D.Y.H.; Yudhistira, I.; Hu, B.Y.-K.; Adam, S. Theory of Coulomb drag in spatially inhomogeneous 2D materials. *Commun. Phys.* **2018**, *1*, 41. [[CrossRef](#)]
9. Kim, S.; Jo, I.; Nah, J.; Yao, Z.; Banerjee, S.K.; Tutuc, E. Coulomb drag of massless fermions in graphene. *Phys. Rev. B* **2011**, *83*, 161401. [[CrossRef](#)]
10. Kamenev, A.; Oreg, Y. Coulomb drag in normal metals and superconductors: Diagrammatic approach. *Phys. Rev. B* **1995**, *52*, 7516. [[CrossRef](#)]
11. Sierra, M.A.; Sánchez, D.; Jauho, A.-P.; Kaasbjerg, K. Fluctuation-driven Coulomb drag in interacting quantum dot systems. *Phys. Rev. B* **2019**, *100*, 81404. [[CrossRef](#)]
12. Zhou, C.; Guo, H. Coulomb drag between quantum wires: A nonequilibrium many-body approach. *Phys. Rev. B* **2019**, *99*, 35423. [[CrossRef](#)]
13. Jauho, A.-P.; Smith, H. Coulomb drag between parallel two-dimensional electron systems. *Phys. Rev. B* **1993**, *47*, 4420. [[CrossRef](#)] [[PubMed](#)]
14. Keller, A.J.; Lim, J.S.; Sánchez, D.; López, R.; Amasha, S.; Katine, J.A.; Shtrikman, H.; Goldhaber-Gordon, D. Cotunneling drag effect in Coulomb-coupled quantum dots. *Phys. Rev. Lett.* **2016**, *117*, 66602. [[CrossRef](#)]
15. Doan, M.-H.; Jin, Y.; Chau, T.K.; Joo, M.-K.; Lee, Y.H. Room-Temperature Mesoscopic Fluctuations and Coulomb Drag in Multilayer WSe₂. *Adv. Mater.* **2019**, *31*, 1900154. [[CrossRef](#)]
16. Gorbachev, R.V.; Geim, A.K.; Katsnelson, M.I.; Novoselov, K.S.; Tudorovskiy, T.; Grigorieva, I.V.; MacDonald, A.H.; Morozov, S.V.; Watanabe, K.; Taniguchi, T.; et al. Strong Coulomb drag and broken symmetry in double-layer graphene. *Nat. Phys.* **2012**, *8*, 896. [[CrossRef](#)]
17. Liu, X.; Wang, L.; Fong, K.C.; Gao, Y.; Maher, P.; Watanabe, K.; Taniguchi, T.; Hone, J.; Dean, C.; Kim, P. Frictional magneto-Coulomb drag in graphene double-layer heterostructures. *Phys. Rev. Lett.* **2017**, *119*, 56802. [[CrossRef](#)]
18. Nandi, D.; Finck, A.D.K.; Eisenstein, J.P.; Pfeiffer, L.N.; West, K.W. Exciton condensation and perfect Coulomb drag. *Nature* **2012**, *488*, 481–484. [[CrossRef](#)]
19. Seamons, J.A.; Morath, C.P.; Reno, J.L.; Lilly, M.P. Coulomb drag in the exciton regime in electron-hole bilayers. *Phys. Rev. Lett.* **2009**, *102*, 26804. [[CrossRef](#)]
20. Yamamoto, M.; Stopa, M.; Tokura, Y.; Hirayama, Y.; Tarucha, S. Negative Coulomb drag in a one-dimensional wire. *Science* **2006**, *313*, 204. [[CrossRef](#)]
21. Raikh, M.E.; von Oppen, F. Coulomb drag for strongly localized electrons: A pumping mechanism. *Phys. Rev. Lett.* **2002**, *89*, 106601. [[CrossRef](#)] [[PubMed](#)]
22. Kozub, V.I.; Galperin, Y.M. Coulomb Drag in Mesoscopic Hopping Insulators. *J. Low Temp. Phys.* **2020**, *198*, 209–223. [[CrossRef](#)]
23. Chou, Y.-Z. Localization-driven correlated states of two isolated interacting helical edges. *Phys. Rev. B* **2019**, *99*, 45125. [[CrossRef](#)]
24. Fetherolf, J.H.; Golež, D.; Berkelbach, T.C. A unification of the Holstein polaron and dynamic disorder pictures of charge transport in organic crystals. *Phys. Rev. X* **2020**, *10*, 21062. [[CrossRef](#)]
25. Troisi, A. Charge transport in high mobility molecular semiconductors: Classical models and new theories. *Chem. Soc. Rev.* **2011**, *40*, 2347–2358. [[CrossRef](#)]
26. Fröhlich, H. Theory of the superconducting state. *Phys. Rev. Lett.* **1950**, *79*, 845.
27. Debray, P.; Zverev, V.N.; Gurevich, V.; Klesse, R.; Newrock, R.S. Coulomb drag between ballistic one-dimensional electron systems. *Semicond. Sci. Technol.* **2002**, *17*, R21. [[CrossRef](#)]
28. Tsukagoshi, K.; Alphenaar, B.W.; Nakazato, K. Operation of logic function in a Coulomb blockade device. *Appl. Phys. Lett.* **1998**, *73*, 2515–2517. [[CrossRef](#)]
29. Amlani, I.; Orlov, A.O.; Snider, G.L.; Lent, C.S.; Bernstein, G.H. Demonstration of a six-dot quantum cellular automata system. *Appl. Phys. Lett.* **1998**, *72*, 2179–2181. [[CrossRef](#)]

30. Baranovskii, S.D. Theoretical description of charge transport in disordered organic semiconductors. *Phys. Status Solidi B* **2014**, *251*, 487–525. [[CrossRef](#)]
31. Franchini, C.; Reticcioli, M.; Setvin, M.; Diebold, U. Polarons in materials. *Nat. Rev. Mater.* **2021**, *6*, 560–586. [[CrossRef](#)]
32. Marcus, R.A. Theory of oxidation-reduction reactions involving electron transfer. Part 4.—A statistical-mechanical basis for treating contributions from solvent, ligands, and inert salt. *Disc. Faraday Soc.* **1960**, *29*, 21–31. [[CrossRef](#)]
33. Hulea, I.N.; Fratini, S.; Xie, H.; Mulder, C.L.; Iossad, N.N.; Rastelli, G.; Ciuchi, S.; Morpurgo, A.F. Tunable Fröhlich polarons in organic single-crystal transistors. *Nat. Mater.* **2006**, *5*, 982. [[CrossRef](#)] [[PubMed](#)]